REGULAR PAPER

Experimental investigation on droplet evaporation characteristics during combustion of future and current aviation fuels with range of properties

L. Zheng[1], C. Wei[2] , Y. Zhang[3] and B. Khandelwal[2]

[1]Department of Mechanical Engineering, Nanjing Institute of Technology, Nanjing, Jiangsu, China, [2]Department of Mechanical Engineering, The University of Alabama, Tuscaloosa, AL, USA and [3]Department of Mechanical Engineering, The University of Sheffield, Sheffield, UK
Corresponding author: B. Khandelwal; Email: bhupendra.khandelwal@gmail.com

Abstract

Currently there is lack of knowledge on how new types of alternative fuels and their storage conditions change the droplet evaporation characteristics. Liquid fuel is commonly stored in wide varieties of containers, where fuel characteristics may change because of the exposure to the material of the container. This study evaluates the impact of different storage containers on droplet evaporation characteristics of different fuels. It was found that there is a distinct phase transition between high volatility to low volatility phase in each fuel stored in steel drums verses fuel that is stored in plastic drums. The type of fuel contaminated by polymer additive has a high impact on fuel droplet burn rates. Polymer additives also have an impact on nucleate boiling, sub-droplets and soot particles. The burning rate constant, K, of selected pure aromatics, various fuel mixtures and Jet A with different cetane numbers have been evaluated. Research has shown that in the low volatility combustion phase a trend reduction of lowest boiling point pure aromatic burning rate to the highest boiling point pure aromatic burning rate is obvious. Irregular change in droplet diameter between the high volatility phase and low volatility phase during the combustion of aromatics blend was observed. This work has also evaluated the relationship between burning rates and cetane numbers.

Nomenclature

Symbol	Unit	Quantity
c_{pg}	$kJ/kg \cdot K$	Constant-pressure specific heat
D_0	mm	Initial diameter of droplet
k_g	$W/m \cdot K$	Thermal conductivity
X_F	pixel	Size of the SiC fibre in the image
X_{im}	pixel	Corresponding value in the image
ρ_l	kg/m^3	Density
B	–	Spalding transfer number
D	mm	Diameter of droplet
DCN	–	Derived cetane number
K	mm^2/s	Burning rate constant
t	s	Time

1.0 Introduction

There are four processes of liquid fuel combustion: fuel atomises forming droplets; the initiation of droplet evaporation; formation of a combustible mixture from the evaporated droplet vapor; and the combustion of said mixture [1]. Liquid fuel is required to be atomised for fuel to burn efficiency in a combustion chamber. The process of atomisation of the liquid fuel is generally accomplished by injecting the fuel or by mixing the fuel with high pressure air or gas [2]. Atomised fuel combustion has an exchange of heat, mass, momentum and chemical reactions simultaneously. The obvious complexity of these processes and interactions increases the difficulty of studying atomization combustion [3–5]. Therefore, droplet combustion is a good way to study liquid fuel combustion [6, 7]. Rasid and Zhang [8] mentioned that during the evaporation of a neat fuel droplet there are three common combustion phases which are the hearing phase, boiling phase and a disruptive phase. Nomura et al. [9] experimentally investigated the mechanism of flame spread along fuel droplet array where they noted that for the multicomponent fuel droplets, the liquid phase process is extremely important to determine the behaviour of the entire fuel droplet's combustion process [10]. There are no chemical reactions that occur in the multicomponent fuel, so each component maintains their own physical and chemical characteristics, such as boiling points and evaporation rates. Both interior heat and mass transfer occur in combustion and evaporation of multicomponent fuel droplets. These characteristics introduce more complexity and uncertainty during the multicomponent fuel droplet combustion processes, as compared to the single component fuel droplet combustion processes.

It has been shown that expansion, ejection and micro-explosion behaviours consistently happen during multicomponent droplet combustion [11, 12]. The occurrence of puffing and micro-explosion directly impacts the overall combustion behaviour of the fuel droplets [13]. Faik and Zhang [10] explained different behaviours, such as generation of bubbles, micro-explosion and atomisation of different diesel base multicomponent droplets during the combustion process. Antonov et al. [14] investigated the expansion and micro-explosion of rapeseed oil/water droplets placed in ethanol as well as a propane/butane mixture flame. They concluded that the amount of time to puffing/micro-explosion of propane/butane mixture flame was always shorter than with an ethanol flame. Faik and Zhang [15] studied binary fuel droplet combustion and showed that interacting fuel droplets have higher nucleation rates than with corresponding isolated fuel droplets. Also, the study found that the relationship between nucleation rate and additive concentration is inversely proportional. Meng et al. [16] pointed out the relationship among micro-explosion, temperature and oxygen, as well as combustion efficiency and micro-explosion intensity of different droplets. Due to the water-fuel mixture allowing the reduction of harmful emissions and improving fuel efficiency, many researchers have conducted research on water fuel emulsions [17–21]. Different models on puffing/micro-explosion, heating and evaporation of water-fuel emulsion droplets have been developed [22–24].

Conventional jet fuels have between 20% and 25% concentration of aromatics by mass. Various engine parts require aromatics in the jet fuels to achieve seals compatibility [25, 26], and required energy density per unit volume. Although aromatics are an important part of the fuel system, they are also responsible for majority of the PM emissions from liquid fuel combustion [27, 28]. Different aromatic species typically produce different amounts of PM emissions, so it is important to complete a comprehensive analysis of different aromatics to achieve both low PM emissions and fuel system component compatibility [29]. Research has been conducted that specifically focused on the aromatic fuel combustion and sprays. Singh et al. [30] studied the emissions of dearomatised hydrocarbon solvent mixed with particular type of aromatic species. Sabourin et al. [31] experimentally studied auto ignition of n-paraffins and n-alkyl aromatics mixtures, then designed a continuous mixture droplet ignition model based on an existing droplet evaporation model. Wijesinghe and Khandelwal [32] investigated spray and atomisation characteristics of different aromatic species mixed with a base blend. Moriue et al. [33] experimentally studied the spontaneous ignition of n-decane dilution by aromatic hydrocarbon droplets and suggested volatility of each component dependence should be considered when applied to spray ignition problems. It can be observed from the above discussion that there are studies in literature that

have investigated the impact of difference in fuel properties on droplet combustion. Though how different aromatic species burn in droplet combustion is still an area which needs further investigation.

Contaminations have significant impact on the fuel droplet combustion. The use of bio-oil as an additive helps to generate slightly decomposed substances that initiate polymerisation and form residues [34]. Rasid and Zhang [35] conducted a study on combustion and ignition of soot contamination on the surface of a diesel fuel droplet and concluded that soot particles on the droplet surface can significantly reduce the evaporation rate and disrupt droplet behaviour throughout its lifetime. Following the investigation on combustion characteristics of soot contamination on the surface of diesel fuel droplet, Rasid and Zhang [36] also studied the combustion behaviour of homogeneous distribution of soot particles in the diesel fuel droplet. They found that the burning rate of contaminated droplets is smaller than neat droplets, and that burning rates can be slightly improve when the loading of soot particles is 0.2% by mass. Polymer addition to fuel has been studied by different researchers, and its impact on droplet combustion has been preliminarily explored. Wang et al. [37] found that polymer addition in a fuel changed the fuel's characteristic to a multicomponent fuel. Singh et al. [38] experimentally evaluated the impact of carbon-based nanoparticles in crude oil droplets. Results show that the addition of carbon-based nanoparticles can decrease the vaper pressure of crude oil droplets but increase bulk heat conductivity and radiation absorption. Some researchers have shown that the addition of polymers to hydrocarbon fuels imparts non-Newtonian properties to the fuel, thereby suppressing splash behaviour when spilling over surfaces [39, 40]. Hazart et al. [41] experimentally studied the emissions produced by combustion of polymer additive biodiesel fuel and it was shown that CO emissions were reduced when polymer additive biofuel was used as compared to no additive case. It was also said that polymer blended fuels might be used as a new clean fuel source. David et al. [42] investigated the effects of mist control of aviation fuel with polymeric additive and found that associative polymers could improve antimisting. Ghamari and Ranter [39] found that at early stages of fuel droplet combustion, polymer additive could reduce evaporation rate, increase swelling behaviours, which eventually reduced the burning time of diesel and jet fuel droplets. Investigations into fuels with polymer addition has been done, although there is a lack of understanding how these fuels will perform under droplet combustion.

Liquid fuel is commonly stored in different types of containers. Plastic drums are suitable for a wide range of materials and are low cost, so they are one of the most versatile containers used for industrial storage and transportation needs. One of the biggest problems is that if liquid fuel is stored in plastic drums, plastic could react with fuel and break down. The polymer-based plastic in the plastic drums readily interact with the fuel. So, fuel storage in plastic or steel drums with polymer lining may change its characteristics by adding polymeric content from the containers into the fuel. All of the above discussed studies on polymer additive have focused on the intentional addition of polymers to fuels. There is no research in literature about impact of polymer contaminated fuel by storage in plastic drums. One of the main objectives of present study is to investigate the impact of polymer contaminated alternative fuels, including pure aromatics and other various multicomponent fuels on droplet evaporation during the combustion.

2.0 Methodology

2.1 Droplet lifetime and combustion phases

The droplet evaporation and combustion model used in this analysis is the classical theory (also known as D^2-law) of droplet combustion designed by Godsave [43] and Spalding [44] in 1953 [45]. The theory exemplifies the essential physics and gives an elementary speculation on droplet regression rate [46] and is still widely used in various research on droplet combustion [45].

In this study, measurement of the burning rate of a fuel droplet is in accordance with D^2-law, which stated that a squared diameter of fuel droplet through its lifetime produced a linear slope that is measured as burning rate constant, K (mm^2/s). K is calculated by the terms of fuel properties and the transfer number, expressed as [46]:
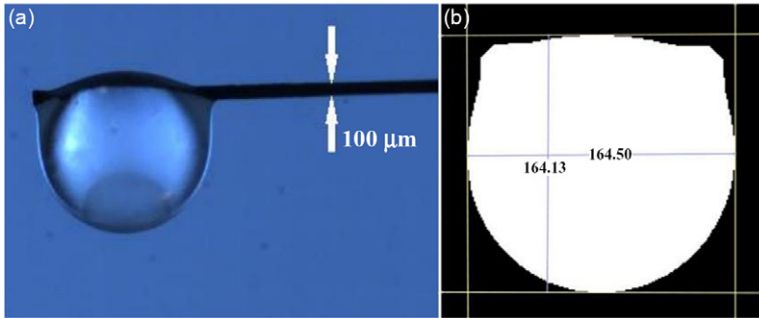
Figure 1. *(a) The original image of droplet and fibre with fixed size; (b) Morphological binary image of droplet.*

$$K = \frac{8k_g}{\rho_l c_{pg}} \ln[1 + B] \tag{1}$$

Where, k_g is Thermal conductivity (W/m · k); ρ_l is Density (kg/m³); c_{pg} is Constant-pressure specific heat (kJ/kg · K); B is the Spalding transfer number.

For the steady burning state, K is a constant to represent the slope of the droplet size variation with time. Hence, the general equation of the temporal droplet size variation (D^2-law) is expressed as:

$$D^2(t) = D_0{}^2 - Kt \tag{2}$$

Where, D is the diameter of droplet, D_0 is the initial diameter of droplet; t is time.

Figure 1(a) shows the original image of droplet and fibre while Fig. 1(b) shows the morphological binary image of the droplet. The image has been improved to make it easier determine boundary line and extract the size features of droplets more accurately. Transferring the color image into the morphological mode has been done through a series of the image processing steps. The calibration of mapping between digital and real dimensions has been done before the experiment. The real size of any droplet is calibrated in accordance with the hanging fibre size, shown as Equation (3).

$$D = 100 * 10^{-3} \frac{X_{im}}{X_F} \tag{3}$$

Where: D is the real value of the droplet (mm); X_{im} is the corresponding value in the image (pixel); X_F is the size of the SiC fibre in the image (pixel).

The actual droplet diameter has been converted as per Equation (3) with the reference to the scale. SiC fibre of known size (10^{-3}mm) is used as reference scale to determine the value of X_F, shown in Fig. 1(a). In this experiment, the average value of the measured transverse, and longitudinal data is taken as the calculated diameter of the droplet (X_{im}). For example, the resolution of the droplet is shown in Fig. 1(b), there are 164.50 pixels in the horizontal direction and 164.13 pixels in the vertical direction, the average pixels number X_{im} is 164.32. By calculation, spatial resolution is 10μm/pixel. Therefore, the actual size of the droplet (D) in this example is 1.6432mm. All the camera setting and spatial resolution data has been listed in Table 1.

Several combustion phases were observed throughout the lifetime of the combusted fuel droplets. Specifically, a binary fuel mixture will have a few additional phases of combustion behaviour as shown in Fig. 2. To facilitate the comparison of different droplet sizes, based on the D^2-law analysis, the droplet size is normalised for the initial droplet size $(D/D_0)^2$ and the time is normalised to the initial droplet size squared $t/(D_0)^2$.

It can be observed in Fig. 2 that the squared droplet diameter is continuously reduced through the passing of time while the slope of the plot changes. Therefore, according to the droplet burning stage,

Table 1. *Camera setting and spatial resolution data*

Frame rate (fps)	Exposure time (μs)	Image resolution (pixel)	Spatial resolution (μm/pixel)	Initial diameter of droplet (mm)
40,000	25	320×240	10	1.1–1.3
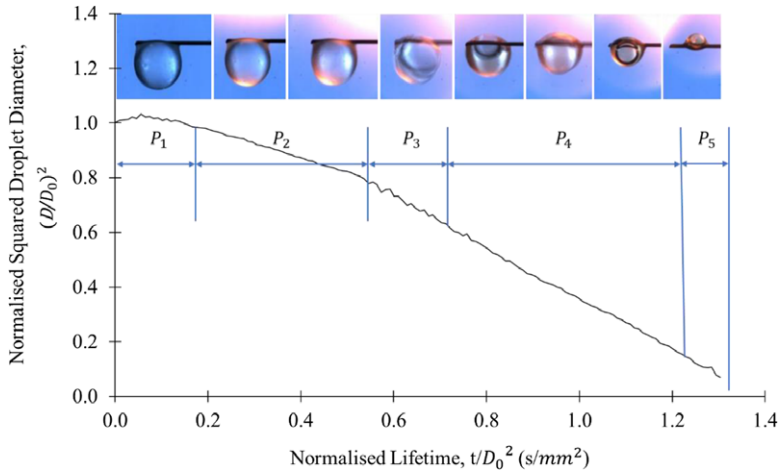
Figure 2. *Binary fuel droplet phases throughout its lifetime during combustion process based on D^2-law analysis.*

after ignition, the droplet combustion state is divided into five phases (P1 to P5). The specific combustion states and the associated behaviours are shown in Table 2.

2.2 Experiment setup

A Photron-SA4 high-speed color camera with Nikon AF Micro NIKKOR 60mm f/2.8D lens was used for the tracking of the lifetime and dynamics of the droplet. Backlighting was incorporated in this experiment to track the size and sharp edge data of the transparent droplets. The backlit imaging was performed by placing a high-intensity light source (IDT 19-LED) with a light diffuser behind the droplet. The images for this study were recorded with a frame rate of 40,000fps. Heated thermal Kanthal wire was placed 1mm below the surface of the liquid drop, and the surrounding ambient air is rapidly heated to 800°C. At this time the droplet exceeds the ignition temperature where it can be ignited without smoke contamination. When the droplet flame is formed, the hot filament is removed quickly to avoid affecting the normal combustion state of the droplet. The overall experimental arrangement is shown in Fig. 3.

For each test, the initial diameters of droplets are kept at 1mm with a measured standard deviation of 0.05mm. The images (in TIFF format) were recorded between the activation of the ignition and the extinguishing of the flame. MATLAB was used to process these images.

2.3 Selected fuels and properties

To determine the impact of polymer contamination on droplet combustion, a number of fuels were selected, and the fuel details are listed in Table 3. Fuels are separated into two categories based on their storage types: plastic or steel. Both sets of drums were stored indoors in dry and cool conditions with no exposure to sunlight for three months prior to testing. Actual pictures of fuel drums storage are shown in Fig. 4. The plastic drums used in this study were being sold on the market as suitable for fuel storage.

Table 2. *Description of combustion phases in the combustion process of binary fuel droplet*

Phases (P)	Behaviour
Droplet heating (P1)	Thermal expansion of fuel droplet. Ignition was observed once the surrounding ambient temperature reached the auto-ignition temperature of the evaporated gas from the droplet.
Higher volatility element combustion (P2)	Once the droplet temperature reaches its boiling temperature, the burning rate stabilizes to a linear slope. For a binary fuel mixture, a higher volatility fuel element controls the combustion behavior thus produced the first linear slope similar to the burning rate of the fuel in its pure form.
Binary element combustion (P3)	Once the fraction of higher volatility fuel is reduced to a small portion, the combustion behavior enters a binary combustion phase. A distinct linear slope would be produced in this phase if the mixture composition is almost equal in terms of weight and large differences in volatility
Lower volatility element combustion (P4)	Once the higher volatility fuel element is almost completely consumed, a linear slope of combustion phase is produced; similar to the lower volatility fuel burning rate in its pure form.
Decomposition (P5)	Due to the suspension of the droplet on SiC fiber, the agglomeration of the combustion products deposits on the fibre and at the same time thicken the droplet. Unstable burning behaviour was presented and unreliable for burning rate measurements due to process of heterogeneous combustion.
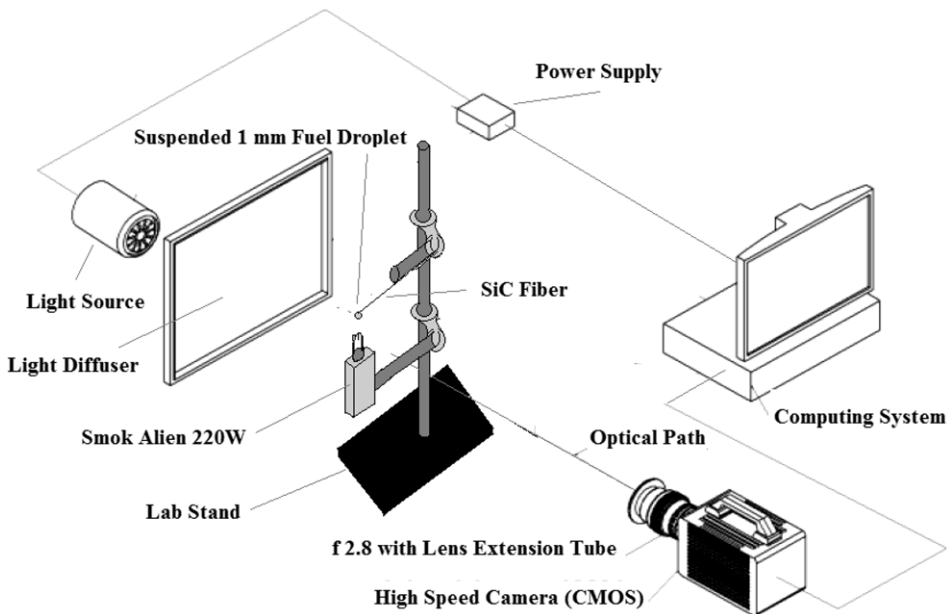
Figure 3. *Experimental setup in high-speed imaging of fuel droplet combustion.*

Table 3. *Fuel stored in steel drum and fuel stored in plastic drum*

Label	Fuel composition	Fuel storage
AR-1A	92% Bannersol, 8% Toluene	Plastic
AR-1A	92% Bannersol, 8% Toluene	Steel
AR-1B	87% Bannersol, 13% Toluene	Plastic
AR-1B	87% Bannersol, 13% Toluene	Steel
AR-1C	82% Bannersol, 18% Toluene	Plastic
AR-1C	82% Bannersol, 18% Toluene	Steel
A2	Jet A	Plastic
A2	Jet A	Steel

Figure 4. *Test fuel batches: plastic (left), steel (right).*

The material of the plastic drums is HDPE, and it was rated for UN Rated 3H1. The steel drums used in this study were lined and approved for fuel storage.

Table 4 shows the selected aromatics used in this experiment. The aim is to determine the burning rate constant of selected aromatics droplet. Table 5 shows various multicomponent and cetane number of Jet A fuels used in this experiment, in purpose of measuring their burning rates.

3.0 Results and discussion

3.1 Droplet combustion characteristics of fuel stored in steel and plastic drum

Figure 5 shows the evolution of diameter squared of fuel stored in steel drum and fuel stored in plastic drum. In each multicomponent and contaminated fuel, there is a distinct phase transition from high volatility (P2) to low volatility (P4) phase. This effect is clearly illustrated in the contaminated Jet A fuel sample, which produced two slopes of combustion phases – with a high volatility and low volatility combustion phases. In P2 stage, there is no obvious difference between the fuels stored in the two containers; however, in P4 stage, the burning lifetime of the fuels stored in the plastic containers can be prolonged significantly. Especially in AR-series fuel products, the higher the mixing degree of Toluene, the more obvious the difference of droplet size. However, Jet A did not show significant difference when stored in plastic drums as compared to steel drums. It indicates that some fuel components are more sensitive to contamination in plastics.

Figures 6 and 7 shows the burning rate constant of tested fuels in high volatility (P2) and low volatility (P4) combustion phases, respectively. It can be observed from Fig. 6 that burning rate constant has

Table 4. *Aromatics fuel samples*

Label	Chemical name
Toluene	Methylbenzene
O-Xylene	1,2-Dimethylbenzene
a-Methystyrene	Phenylpropene
Pseudocumene	1,2,4-Trimethylbenzene
Tetralin	1,2,3,4-Tetrahydronapthalene
TertButylbenzene	2-Methyl-2-phenylpropane

***Table 5.*** *Various multicomponent fuels and Jet A with different cetane number*

| Label	Fuel composition	Fuel condition
C7	RP-2 (75 vol%), A-3 (23 vol %), Penn State high decalin (2%)	High cycloparaffin
C8	Jet A + Exxon aromatic blend	High aromatic
C9	R-8 HEFA (80 vol%), n-dodecane (20 vol%)	High derived cetane
31 FP	Jet A	30–32 Cetane
44 FP	Jet A	45 Cetane
54 FP	Jet A	55 Cetane
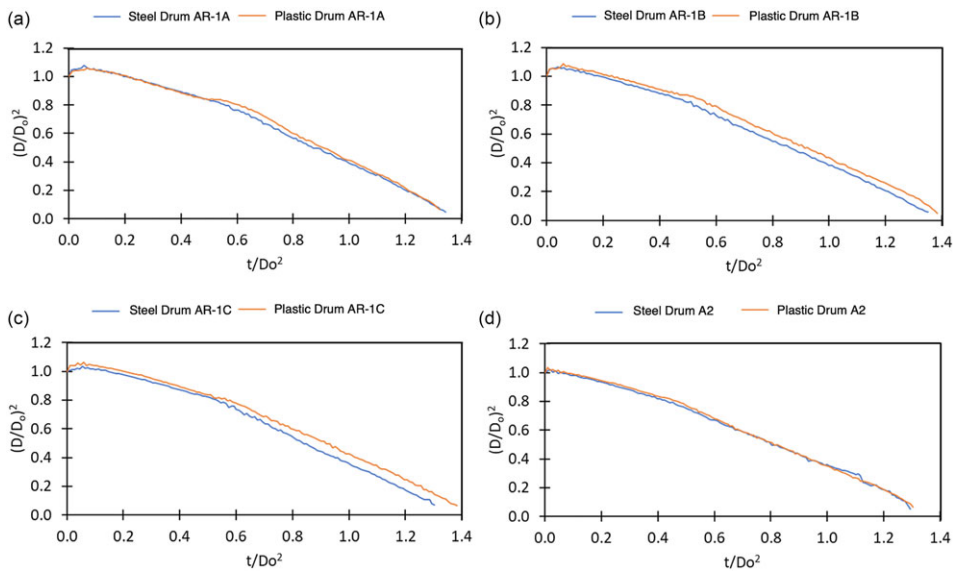
Figure 5. *Evolution of diameter square of fuel stored in steel drum and fuel stored in plastic drum for (a) AR-1A, (b) AR-1B, (c) AR-1C and (d) A2.*

changed in high volatility (P2) phase when the fuel is stored in plastic drums as compared to steel drums. For the steel drums, with increasing content of Toluene the burning rate constant at high volatility (P2) phase has decreased, and for plastic drum case it has increased. This change in P2 stage could be due to the fact that Toluene is an aromatic hydrocarbon, and its molecular bond is relatively stable compared with Bannersol during combustion. Therefore, theoretically, with the increase of T content, the combustion rate should be lower. The combustion rate of AR series fuels stored in steel drums shows a decreasing trend, which basically conforms to the normal theoretical cognition. The fuel in the plastic
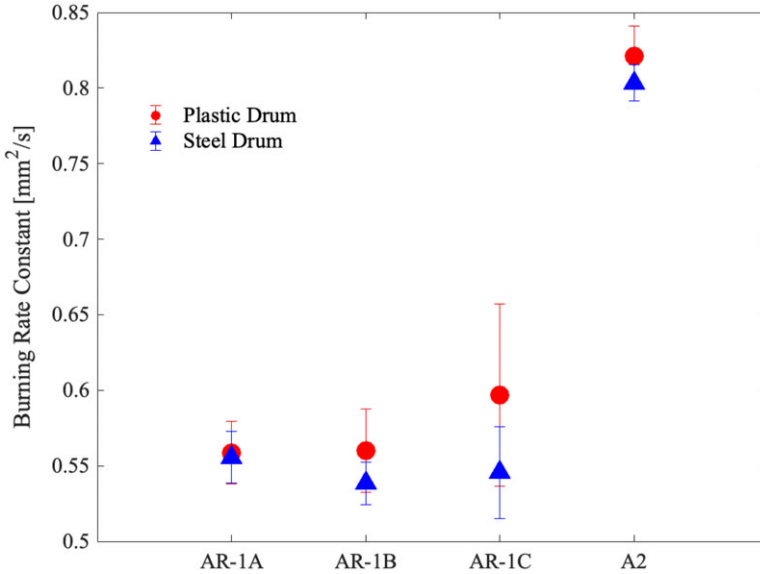
Figure 6. *Burning rate constant, K in high volatility combustion phase (P2) of fuel stored in steel drum and fuel stored in plastic drum. The error bars show standard deviation.*
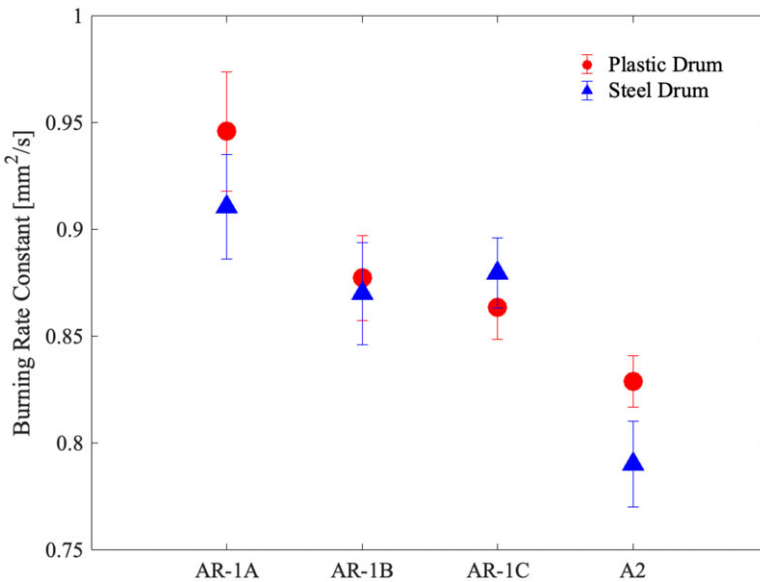
Figure 7. *Burning rate constant, K in low volatility combustion phase (P4) of fuel stored in steel drum and fuel stored in plastic drum. The error bars show standard deviation.*

drums shows a completely opposite trend to that expected. Therefore, it indicates that impurities in the plastic drum may change its chemical properties and cause this unexplained result.

At the P4 stage, in general, burning rate constant in P4 is higher than in P2. Regardless of the term 'low volatility', higher burning rate in these phases were due to its higher boiling point of the components, thus increased the droplet temperature and evaporation rate in the process. All fuels follow the rule that
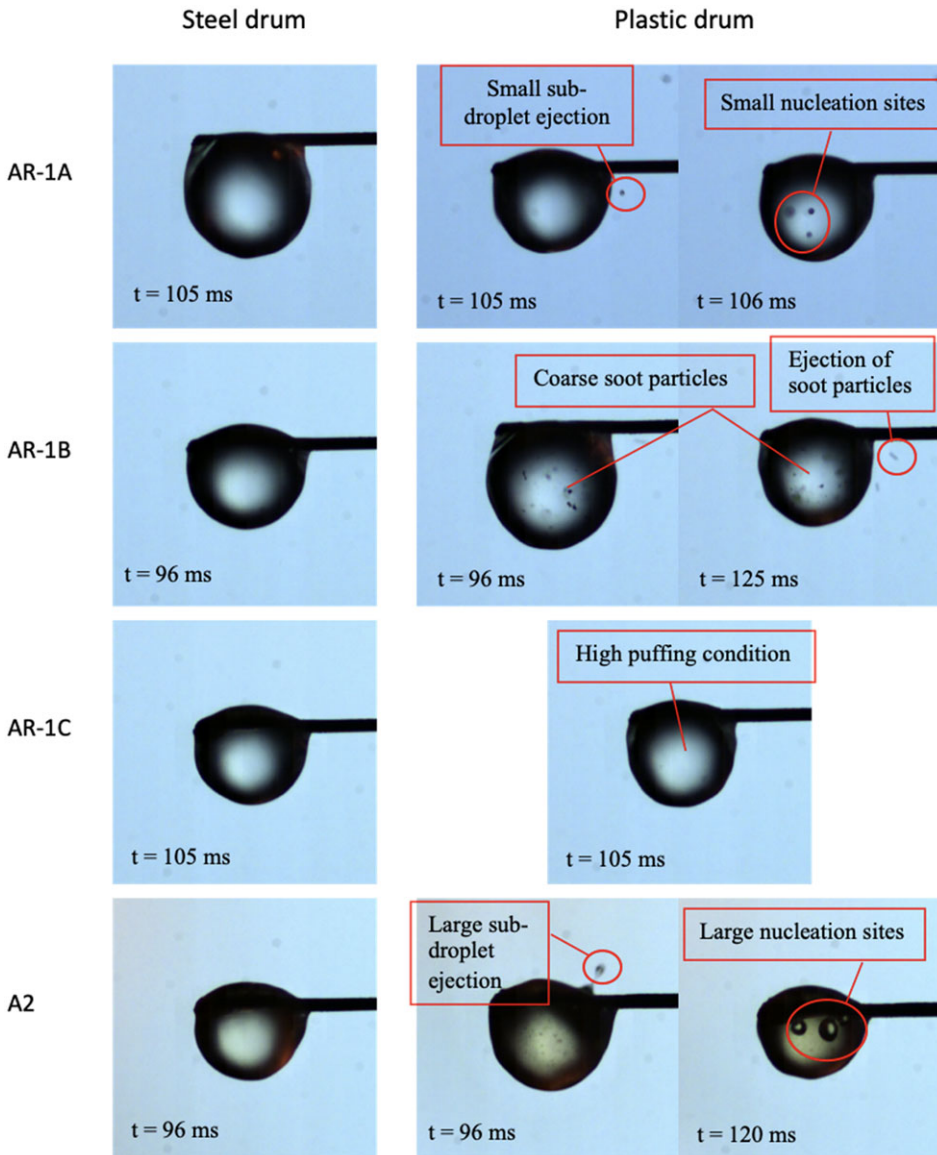
Figure 8. *Liquid phases of fuel stored in steel drum and fuel stored in plastic drum in low volatility combustion phase.*

the combustion rate decreases with the increase of aromatic hydrocarbons. In addition, the uncertainty is also reduced. This indicates that with the increase of droplet temperature, the impact of burning rate caused by pollution from plastic drums is alleviated. This means that if burning in the engine, the impact of plastic drum pollution on the fuel may not be obvious at high temperature or rich fuel combustion stage, but it will have a greater impact at low temperature or lean fuel burning and ignition.

Test done by Ghamari and Ratner [39] showed that polymer contamination in Jet-A has low effect on the burning rate reduction in volatile phase combustion compared to diesel fuel. This shows that changes in the burning rate of the fuel is highly dependent on the type of fuel contaminated by polymer

Tetralin	Terbutylbenzene	a-Methystyrene	Pseudocumene	O-Xylene	Toluene
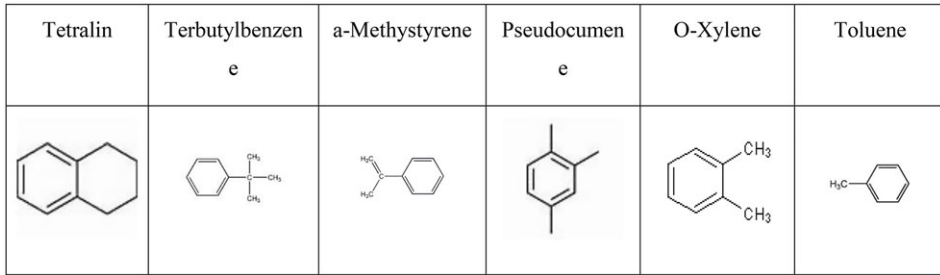
Figure 9. *Evolution of diameter square of pure aromatics and bannersol.*
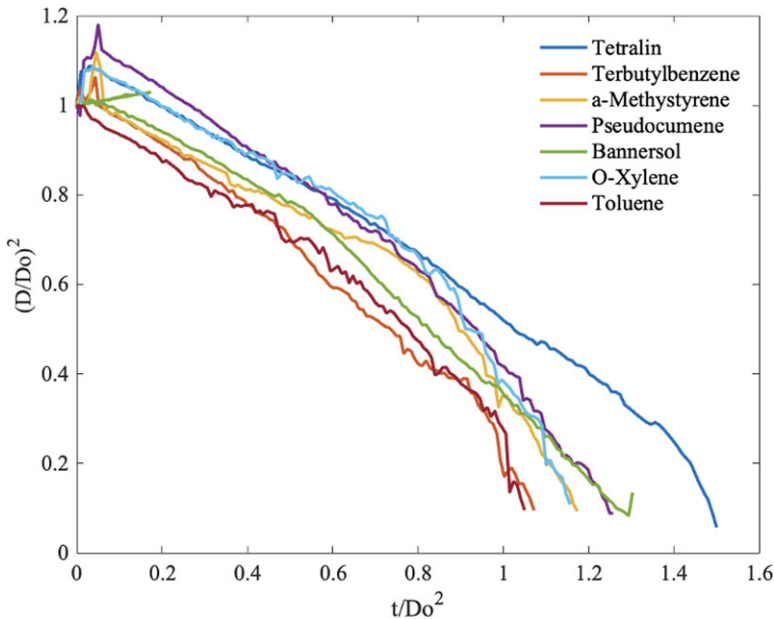
Figure 10. *Different aromatic species droplet phases throughout its lifetime during combustion process based on D2-law analysis.*

additives. From Figs. 6 and 7, it can be observed that Toluene has a stronger dependence on polymer contamination, as fuel with higher Toluene composition has increased the burning rate in high volatility phase.

This justified the result obtained in this test, which has proven that there was an increase in burning rate for contaminated fuels of AR-1A, AR-1b and A2 fuel, higher than their respective fine fuels. During this phase, the composition of polymer contamination was denser, thus increased the evaporation rate due to improved heat conductivity within the fuel droplet.

Polymer has a higher density than both diesel and jet fuel. It also has very low volatility because of a very high boiling point. As droplets continue to evaporate, the mass fraction of polymer increases, which lead to increasing droplet surface temperature to exceed boiling temperature of fuel. Under this condition, polymer will cause the droplets to swell and bubble. An interesting phenomenon revealed by Yang et al. [47] is, during combustion, most of the polymer sphere is made by gaseous bubbles, then bubbles will grow and escape from the polymer, causing sputter.

Figure 8 shows the images of liquid phases of fuel stored in steel drum and fuel stored in plastic drum in low volatility combustion phase. Referring to liquid state of fuel stored in plastic drum in Fig. 8, it was
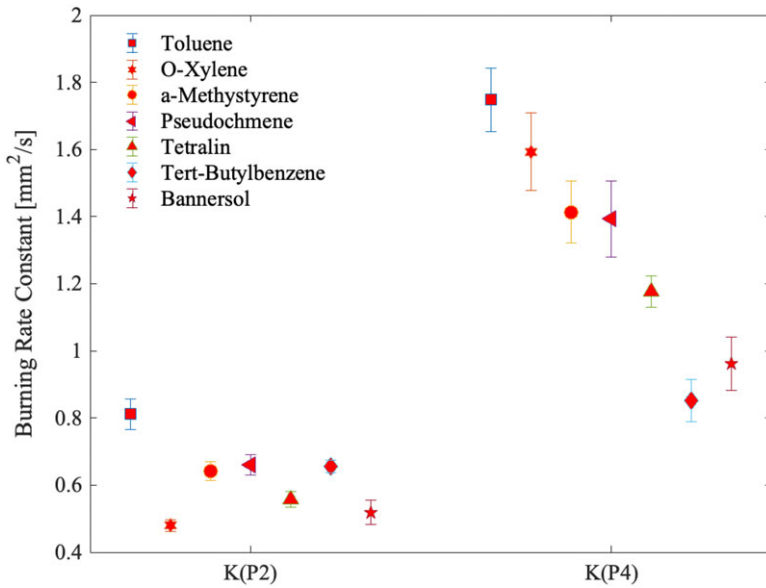
Figure 11. *Burning rate of pure aromatics and bannersol. Error bars show standard deviation.*
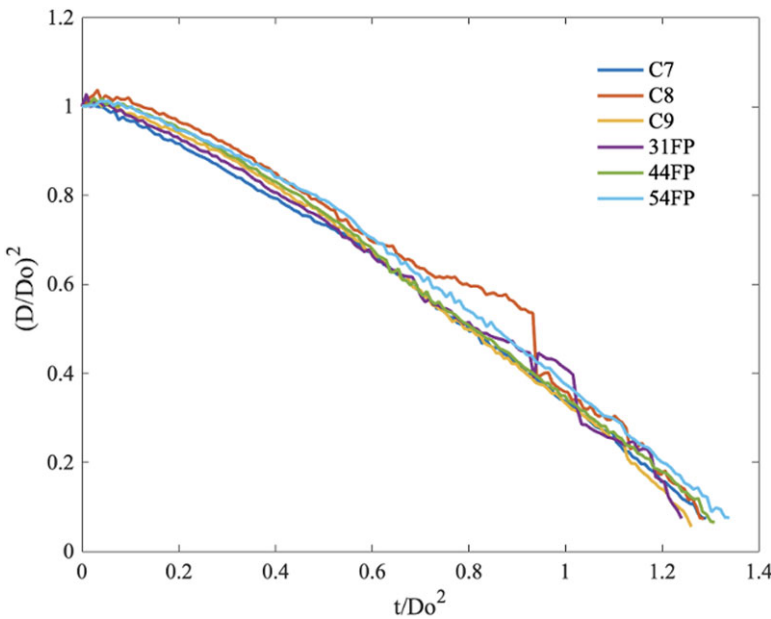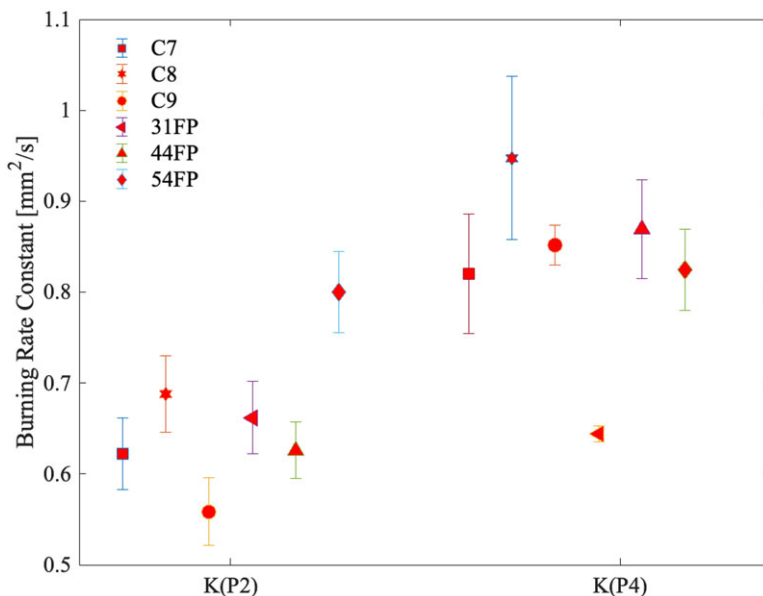

Figure 12. *Evolution of squared diameter of various multicomponent fuels and cetane number of Jet A.*

observed that polymer presence in the fuel played as the nucleation sites that created bubbles emerging from inside the droplet. More active swelling of the droplet was recorded for each contaminated fuel, as higher droplet temperature tends to increase the core temperature and thus increased the fuel temperature, exceeding its boiling temperature and resulting a puffing condition. Referring to the contaminated

Figure 13. *Burning rate of various multicomponent and cetane number of Jet A. The error bars show standard deviation.*

fuels liquid state in Fig. 8, it was observed that polymer presence in the fuel played as the nucleation sites that created bubbles emerging from inside the droplet.

As reported by Ghamari and Ratner [39], soot produced during combustion might be captured by the polymer strings in polymer additive fuel and explains the agglomerations shown in contaminated fuels in Fig. 8. Higher amounts of soot trapped inside the droplet further increased the boiling temperature, thus elevated the fuel temperature beyond its boiling temperature, causing micro shootings of the soot particle and fuel sub-droplets.

3.2 Droplet combustion characteristics of selected aromatics

Figure 9 shows the structure of different aromatic species selected in this study for investigation on droplet combustion characteristics. Figure 10 shows different aromatic species droplet phases throughout its lifetime during combustion process based on D2-law analysis. It can be observed from Figs. 9 and 10 that the biphenyl benzene ring with larger molecules, such as the droplet of Tetralin, is the most difficult to decompose and often burns the longest. On the contrary, some fuels with smaller molecules (branched molecule), such as Toluene and Terbutylbenzene, rapidly decrease in droplet size and burn out. This is an indication that in combustion of aromatics droplet, low volatility phase burns with higher rate due to the breakup of strong molecular chains, thus evaporated the fuel even faster.

Figure 11 compares the combustion rates of different fuels in different combustion stages (P2 and P4). As expected, the burning rate constant, from high to low-rate, correlates with aromatics that possess the lowest boiling point to the highest boiling point. As the fuel with the smallest molecule, Toluene's combustion rate is obviously higher than other fuels in both P2 and P4 stages. The reducing trend of burning rates are obvious in low volatility combustion phase (P4, as they go through chemical compositions). O-Xylene has shown significantly different combustion properties. In P2 stage, O-Xylene combustion rate is the lowest, which even lower than that of bicyclic aromatic hydrocarbons (Tetralin). However, in the P4 stage, its combustion rate is only second to toluene. In terms of the complexity of the molecular chain, its combustion performance should be in the middle position, so this study guesses that in

addition to the factors of volatility and molecular arrangement, there are other physical and chemical characteristics that need to be considered, and further research needs to be carried out.

3.3 Droplet combustion characteristics of various multicomponent fuels

Figure 12 shows droplet evolution of various fuel mixtures. From the chemical composition table, C8 contained aromatics blend. Obvious irregular change in droplet diameter was observed in its combustion behaviour; having a chemical decomposition phase as illustrated in the Fig. 12. Theoretically, for Jet A with distinct DCN values, a rise in cetane number should correspond to an increased combustion rate. However, in this particular experiment, Fig. 13 reveals that no clear trend changes were detected in relation to shifts in DCN.

4.0 Conclusion

Droplet evaporation during the combustion of different alternative and conventional fuels with a range properties and storage conditions have been experimentally investigated in this paper. Selected fuels are divided into three groups. In the first group there are four different fuels. They are stored in plastic drums (approved for fuel storage) and steel drums respectively to determine the impact of storage drums. The second group is made up of seven different pure aromatic species. The third group contains various multicomponent refined fuels and Jet A with different cetane number. For fuels stored in plastic and steel drums, it was observed that combustion properties change when fuel was stored in plastic drums. Plastic drums were found to be contaminating the fuel and it is found that they are more likely to produce unstable phenomena such as soot, jet and bubble, which leads to fuel consumption but not complete combustion. It was also found that the impact of plastic drums contamination on fuel may not be obvious at high temperature combustion or during the rich fuel combustion stage, but it will have greater impact at low temperature or lean fuel combustion and ignition stages. For the pure aromatics, molecular structure, atomic bond stability and volatility jointly impact the combustion rate of droplets. It was observed that smaller molecules and highly volatile fuels burn faster. However, O-Xylene showed different burn rates trends as compared to other aromatic species. Therefore, the influence of other chemical and physical factors is not excluded. For the various multicomponent fuels and Jet A with different DCN, theoretically, with the increase of cetane number, the combustion rate should show an upward trend. However, in this experiment, no obvious trend change with the change of DCN has been observed.

References

[1] Warnatz, J., Maas, U., and Dibble, R.W. *Combustion: Physical and Chemical Fundamentals, Modeling and Simulation, Experiments, Pollutant Formation*, Springer, 2006.

[2] Chigier, N.A. The atomization and burning of liquid fuel sprays, *Prog Energy Combust Sci*, 1976, **2**, (2), pp 97–114.

[3] Xin, J., Ricart, L. and Reitz, R.D. Computer modeling of diesel spray atomization and combustion, *Combust Sci Technol*, 1998, **137**, (1–6), pp 171–194. https://doi.org/10.1080/00102209808952050

[4] Lee, C.S., Park, S.W. and Kwon, S.I., An experimental study on the atomization and combustion characteristics of biodiesel-blended fuels, *Energy Fuels*, 2005, **19**, (5), pp. 2201–2208. https://doi.org/10.1021/ef050026h

[5] Shen, Y., Li, F., Liu, Z., Wang, H. and Shen, J. Study on the characteristics of evaporation–atomization–combustion of biodiesel, *J Energy Inst*, 2019, **92**, (5), pp 1458–1467. https://doi.org/10.1016/j.joei.2018.08.005

[6] Kotake, S. and Okazaki, T. Evaporation and combustion of a fuel droplet, *International Journal of Heat and Mass Transfer*, 1969, **12**, (5), pp 595–609.

[7] Han, K., Yang, B., Zhao, C., Fu, G., Ma, X. and Song, G. Experimental study on evaporation characteristics of ethanol-diesel blend fuel droplet, *Exp Therm Fluid Sci*, 2016, **70**, pp 381–388. https://doi.org/10.1016/j.expthermflusci.2015.10.001

[8] Rasid, A.F.A. and Zhang, Y. Combustion phases of evaporating neat fuel droplet, *J Adv Res Fluid Mech Therm Sci*, 2022, **96**, (1), pp 60–69. https://doi.org/10.37934/arfmts.96.1.6069

[9] Nomura, H., Takahashi, H., Suganuma, Y. and Kikuchi, M. Droplet ignition behavior in the vicinity of the leading edge of a flame spreading along a fuel droplet array in fuel-vapor/air mixture, *Proc Combust Inst*, 2013, **34**, (1), pp 1593–1600. https://doi.org/10.1016/j.proci.2012.05.049

[10] Faik, A.M.D. and Zhang, Y. Multicomponent fuel droplet combustion investigation using magnified high speed backlighting and shadowgraph imaging, *Fuel*, 2018, **221**, pp 89–109. https://doi.org/10.1016/j.fuel.2018.02.054

[11] Lasheras, J.C. and Dryer, F.L. *Effect of the Ambient Pressure on the Explosive Burning of Emulsified and Multicomponent Fuel Droplets*, The Combustion Institute, 1984.

[12] Chausalkar, A., Kweon, C.B.M. and Michael, J.B. Multi-component fuel drop-wall interactions at high ambient pressures, *Fuel*, 2021, **283**, p 119071. https://doi.org/10.1016/j.fuel.2020.119071

[13] Rao, D.C.K. and Karmakar, S. Crown formation and atomization in burning multi-component fuel droplets, *Exp Therm Fluid Sci*, 2018, **98**, pp 303–308. https://doi.org/10.1016/j.expthermflusci.2018.06.007

[14] Antonov, D.V., Fedorenko, R.M., Strizhak, P.A., Nissar, Z. and Sazhin, S.S. Puffing/Micro-explosion in comptosite fuel/water droplets heated in flames, *Combust Flame*, 2021, **233**, p 111599. https://doi.org/10.1016/j.combustflame.2021.111599

[15] Faik, A.M.D. and Zhang, Y. Liquid-phase dynamics during the two-droplet combustion of diesel-based fuel mixtures, *Exp Therm Fluid Sci*, 2020, **115**, p 110084. https://doi.org/10.1016/j.expthermflusci.2020.110084

[16] Meng, K., Bao, L., Li, F., Wang, C. and Lin, Q. Experimental understanding on combustion and micro-explosion characteristics of mixed droplets of aviation fuel, biodiesel and ethanol, *J Energy Inst*, 2021, **97**, pp 169–179. https://doi.org/10.1016/j.joei.2021.03.021

[17] Watanabe, H., Suzuki, Y., Harada, T., Matsushita, Y., Aoki, H. and Miura, T. An experimental investigation of the breakup characteristics of secondary atomization of emulsified fuel droplet, *Energy*, 2010, **35**, (2), pp 806–813. https://doi.org/10.1016/j.energy.2009.08.021

[18] Antonov, D.V., Kuznetsov, G.V., Fedorenko, R.M. and Strizhak, P.A. Ratio of water/fuel concentration in a group of composite droplets on high-temperature heating, *Appl Therm Eng*, 2022, **206**, p 118107. https://doi.org/10.1016/j.applthermaleng.2022.118107

[19] Antonov, D., Piskunov, M., Strizhak, P., Tarlet, D. and Bellettre, J. Dispersed phase structure and micro-eaxplosion behavior under different schemes of water-fuel droplets heating, *Fuel*, 2020, **259**, p 116241. https://doi.org/10.1016/j.fuel.2019.116241

[20] Lasheras, J.C., Fernandez-Pello, A.C. and Dryer, F.L. Initial observations on the free droplet combustion characteristics of water-in-fuel emulsions, *Combust Sci Technol*, 1979, **21**, (1–2), pp 1–14. https://doi.org/10.1080/00102207908946913

[21] Faik, A.M.E.D., Theeb, M.A. and Zhang, Y. Post-impact characteristics of a diesel-in-water emulsion droplet on a flat surface below the leidenfrost temperature, *Int J Renew Energy Dev*, 2021, **10**, (2), pp 297–306. https://doi.org/10.14710/ijred.2021.34036

[22] Nissar, Z., Rybdylova, O., Sazhin, S.S., Heikal, M., Aziz, A.R.B.A. and Ismael, M.A. A model for puffing/microexplosions in water/fuel emulsion droplets, *Int J Heat Mass Trans*, 2020, **149**, p 119208. https://doi.org/10.1016/j.ijheatmasstransfer.2019.119208

[23] Shen, S., Che, Z., Wang, T., Yue, Z., Sun, K. and Som, S. A model for droplet heating and evaporation of water-in-oil emulsified fuel, *Fuel*, 2020, **266**, p 116710. https://doi.org/10.1016/j.fuel.2019.116710

[24] Sazhin, S.S., Rybdylova, O., Crua, C., Heikal, M., Ismael, M.A., Nissar, Z. and Aziz, A.R.B.A. A simple model for puffing/micro-explosions in water-fuel emulsion droplets, *Int J Heat Mass Trans*, 2019, **131**, pp 815–821. https://doi.org/10.1016/j.ijheatmasstransfer.2018.11.065

[25] Almohammadi, B.A., Singh, P., Sharma, S., Kumar, S. and Khandelwal, B. Experimental investigation and correlation development for engine emissions with polycyclic aromatic blended formulated fuels, *Fuel*, 2021, **303**, p 121280. https://doi.org/10.1016/j.fuel.2021.121280

[26] Undavalli, V., Gbadamosi Olatunde, O.B., Boylu, R., Wei, C., Haeker, J., Hamilton, J. and Khandelwal, B. Recent advancements in sustainable aviation fuels, *Progr Aerosp Sci*, 2023, **136**, p 100876.

[27] DeWitt, M.J., Corporan, E., Graham, J. and Minus, D. Effects of aromatic type and concentration in Fischer-Tropsch fuel on emissions production and material compatibility, *Energy Fuels*, 2008, **22**, (4), pp 2411–2418. https://doi.org/10.1021/ef8001179

[28] Zheng, L., Singh, P., Cronly, J., Ubogu, E.A., Ahmed, I., Ling, C., Zhang, Y. and Khandelwal, B. Impact of aromatic structures and content in formulated fuel for jet engine applications on particulate matter emissions, *J Energy Res Technol Trans ASME*, 2021, **143**, (12), p 122301. https://doi.org/10.1115/1.4049905

[29] Sharma, S., Singh, P., Bhardwaj, C., Khandelwal, B. and Kumar, S. Investigations on combustion and emissions characteristics of aromatic fuel blends in a distributed combustor, *Energy Fuels*, 2021, **35**, (4), pp 3150–3163. https://doi.org/10.1021/acs.energyfuels.0c03511

[30] Singh, P., Sharma, S., Almohammadi, B.A., Khandelwal, B. and Kumar, S. Impact of fuel formulation with particular selection of aromatics on compression engine performance and emission control, *AIAA Scitech 2021 Forum, January* 2021. https://doi.org/10.2514/6.2021-1808

[31] Sabourin, S.W., Boteler, C.I. and Hallett, W.L.H. Droplet ignition of approximately continuous liquid mixtures of N-paraffins and n-Alkyl aromatics. *Combust Flame*, 2016, **163**, pp 326–336. https://doi.org/10.1016/j.combustflame.2015.10.008

[32] Wijesinghe, C.J. and Khandelwal, B. Impact of aromatic species selection and micro and bulk properties of alternative fuels on atomization, *Aeronaut J*, 2021, **125**, (1288), pp 1013–1033. https://doi.org/10.1017/aer.2021.6

[33] Moriue, O., Eigenbrod, C., Rath, H.J., Sato, J., Okai, K., Tsue, M. and Kono, M. Effects of dilution by aromatic hydrocarbons on staged ignition behavior of n-decane droplets, *Proc Combust Inst,* 2000, **28**, pp 969–975.

[34] Wu, M.S. and Yang, S.I. Combustion characteristics of multi-component cedar bio-oil/kerosene droplet, *Energy*, 2016, **113**, pp 788–795. https://doi.org/10.1016/j.energy.2016.07.097

[35] Rasid, A.F.A. and Zhang, Y. Combustion characteristics and liquid-phase visualisation of single isolated diesel droplet with surface contaminated by soot particles, *Proc Combust Inst*, 2019, **37**, (3), pp 3401–3408. https://doi.org/10.1016/j.proci.2018.08.023

[36] Abdul Rasid, A.F. and Zhang, Y. Comparison of the burning of a single diesel droplet with volume and surface contamination of soot particles, *Proc Combust Inst*, 2021, **38**, (2), pp 3159–3166. https://doi.org/10.1016/j.proci.2020.07.092

[37] Wang, C.H., Liu, X.Q. and Law, C.K. Combustion and microexpiosion of freely falling multicomponent droplets, *Combustion Flame*, 1984, **56**, pp 175–197.

[38] Singh, G., Esmaeilpour, M. and Ratner, A. Effect of carbon-based nanoparticles on the ignition, combustion and flame characteristics of crude oil droplets, *Energy*, 2020, **197**, p 117227. https://doi.org/10.1016/j.energy.2020.117227

[39] Ghamari, M. and Ratner, A. Combustion characteristics of diesel and jet-a droplets blended with polymeric additive, *Fuel*, 2016, **178**, pp 63–70. https://doi.org/10.1016/j.fuel.2016.03.052

[40] David, R.L.A., Wei, M.H., Liu, D., Bathel, B.F., Plog, J.P., Ratner, A. and Kornfield, J.A. Effects of pairwise, self-associating functional side groups on polymer solubility, solution viscosity, and mist control, *Macromolecules*, 2009, **42**, (4), pp 1380–1391. https://doi.org/10.1021/ma802058s

[41] Hazrat, M.A., Rasul, M.G., Khan, M.M.K., Ashwath, N. and Rufford, T.E. Emission characteristics of polymer additive mixed diesel-sunflower biodiesel fuel, *Energy Proc*, 2019, **156**, pp 59–64.

[42] David, R.L.A., Wei, M.H., Liu, D., Bathel, B.F., Plog, J.P., Ratner, A. and Kornfield, J.A. Effects of pairwise, self-associating functional side groups on polymer solubility, solution viscosity, and mist control, *Macromolecules*, 2009, **42**, (4), pp 1380–1391. https://doi.org/10.1021/ma802058s

[43] Godsave, G.A.E. Studies of the combustion of drops in a fuel spray-the burning of single drops of fuel, *Symp (Int) Combust*, 1953, **4**, (1), pp 818–830.

[44] Spalding, D.B. The combustion of liquid fuels, *Combustion of Liquid Fuels,* 1953.

[45] Choi, M. and Dryer, F.L. Microgravity droplet combustion, In *Microgravity Combustion: Fire in Free Fall* (H. Ross, ed.), 2001, pp 183–297.

[46] Law, C.K. Recent advances in droplet vaporization and combustion, *Progress in Energy and Combustion Science*, 1982, **8**, (3), pp 171–201.

[47] Yang, J.C., Hamins, A. and Donnelly, M.K. Reduced gravity combustion of thermoplastic spheres, *Combust Flame*, 2000, **120**, (1–2), January 2000, pp 61–74.